Correlates of 30-MPH Intersection Collisions

DERWYN M. SEVERY, Research Engineer, Institute of Transportation and Traffic Engineering, University of California, Los Angeles

Two automobile intersection collision experiments were conducted under identical crash conditions to evaluate data reproducibility and provide a basis for studying performance differences accompanying changes in important subvariables. Studies were made of collision performance as a function of whether the cars had been involved in a previous, more severe impact. Comparison of vehicle dynamics, skid and debris patterns, damage patterns, and cost to repair is provided. Average coefficients of friction operating during specific postcontact spin-out trajectories of vehicles were calculated, and related findings discussed. In addition, the difference between laminated and tempered side-window glass for the struck car was evaluated for this particular collision exposure.

Triaxial accelerometers, mounted in the heads and chests of anthropometric dummies, safety belt tensiometers and high-speed photography provided the principal sources of recorded data. An IBM 7090 computer facilitated data reduction. The relative performances of lap belt vs combination shoulder and lap belts were studied for simulated adult motorists; child and infant dummies were used to evaluate special restraining devices.

• DURING a two-year period 14 intersection-type collision experiments were conducted for the purpose of obtaining detailed information on the dynamic interaction between motorist and vehicle structure (Fig. 1). This series of collisions represented 28 car-damage exposures for the six available 1960 Plymouth four-door sedans. It was necessary, therefore, to repair these cars following each collision. Three positions of impact and four speeds of impact were selected to represent intersection collision configurations (Fig. 2). The 30-mph collision into the center doorpost (Experiment 57) was selected for a repeat study for correlation purposes. The relation these experiments, X-57 and X-62, bear to the entire Series II experiments is shown in the figure; the X-57, X-62 impact configuration is shown cross-hatched.

(Experiment 57, or X-57, refers to one of 64 full-scale collision experiments conducted at UCLA during the years between 1949 and 1963. These experiments have been numbered consecutively, starting with Experiment 1 conducted in 1949. The correlate Experiments 57 and 62, reported by this paper, were conducted in 1961 and 1962, respectively.)

At the conclusion of the Series II experiments, X-62 was conducted to obtain data that could be used to establish the correlation of collision dynamics thus obtained with similar data from X-57. This comparison provided data from two 30-mph center-side impact experiments of identical collision configuration, but involving cars having different histories of prior impacts. The striking car for Experiment 57 had not been used previously as a striking car and had been struck at its left front side in a previous 20-mph experiment. The struck car for Experiment 57 had been used as a striking car in a 20-mph rear-side collision and as a struck car in both front-side and rear-side collisions at 10 mph. The procedure of conducting a series of experiments at one speed (for example, 20 mph) and then scheduling each of these cars once again, following re-

Paper sponsored by Committee on Highway Safety Research.

pairs, to a 30-mph impact was based on the postulation that the effect of an earlier low-speed impact on the car's collision performance at a higher speed would be negligible. Both cars used for the 30-mph correlate Experiment 62 had been repaired, following exposure to an earlier 40-mph collision. In addition, these cars had previously been used for 10-, 20-, and 30-mph collisions but, of course, had been repaired following each of these experiments.

This review of collision histories establishes that the prior exposures for the cars used in Experiment 57 were minor compared with the prior exposures of the cars used

Figure 1. Intersection collision.

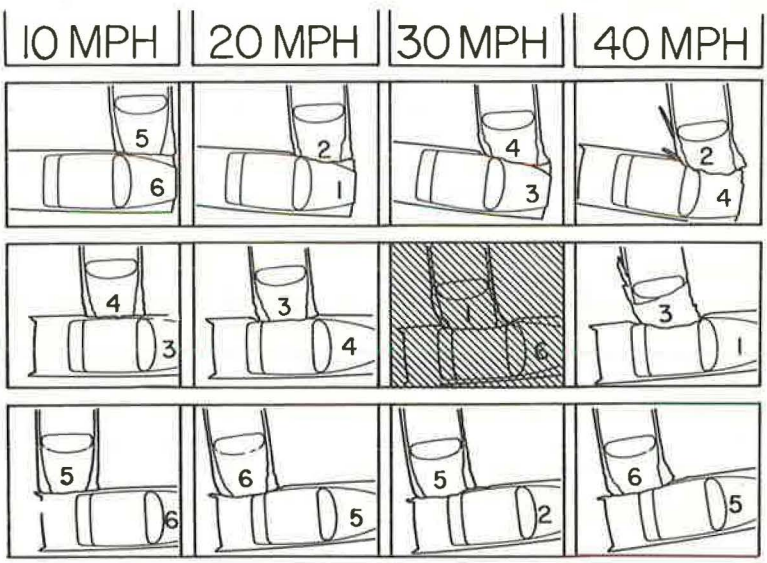

Figure 2. Automobile assignment schedule (correlate Experiments 57 and 62 cross-hatched).

in Experiment 62. The comparative data to be presented from these two experiments show that for right-angle collisions up to 40 mph, a car's collision performance is essentially unimpaired by damage sustained from previous collisions, providing quality repair work has been performed.

Perhaps more important than determining the validity of using repaired vehicles in the Series II experiments was the opportunity that the correlate experiment provided for evaluating other factors. Many occupant environmental conditions could be modified for this correlate experiment without compromising the basic purpose of the experiments.

EQUIPMENT AND FACILITIES

Although described in detail by prior publications (1, 2), a brief explanation of physical facilities and equipment required for these experiments will assist in understanding the discussions of findings to follow. A decommissioned airstrip at the U.S. Naval Station, Long Beach, Calif., was made available by the Navy for UCLA's collision research. On the airstrip's level asphalt surface, an aluminum monorail guide track system was anchored to provide directional control for the crash vehicles. Other operational systems described elsewhere (1, 2) were incorporated, permitting side-impact collision experiments to be conducted under completely controllable and yet absolutely realistic conditions. A mobile electronics laboratory, a mobile machine shop, and an operations van provide on-the-scene research support facilities. The Chrysler Corporation donated the six 1960 Plymouth four-door sedans used as collision cars, two station wagons serving as mobile instrumentation recording vehicles, and a Chrysler Model 300 G as a tow vehicle for accelerating the crash cars to their impact positions. Other equipment and facilities required for this research were provided in part by the University of California and, in substantial measure, by a research grant from the U.S. Public Health Service.

PROCEDURES AND INSTRUMENTATION

A detailed explanation of experimental procedures and instrumentation systems is provided in prior publications (1, 2); however, a brief explanation will assist to a better understanding of the discussion of the findings. A tow car is connected to each of the two crash cars by a steel cable passing around sheaves (Fig. 3). The length of the cable to each crash car is adjusted to assure their proper position at the time of collision. The crash cars receive directional control from their slipper-shoe connection with the monorail guide track they straddle as they are pulled toward the position of impact. Both constraints—the towing and directional control—are released prior to impact. High-speed cameras and other photographic devices are positioned as shown by the black squares in Figure 2; their individual specifications are given in Table 1. In addition, each car and its occupants are instrumented with transducers whose outputs are transmitted to an instrument recording car by way of a 100-ft electrical cable. Each instrument car carried an 18-channel recording oscillograph and remote controls for starting cameras located on the crash cars and to operate the crash car's emergency braking system.

An operation plan is developed for each series of collision experiments and carries an appendix that describes in detail the various phases of preparation necessary before an experiment can be conducted. Only by meticulously adhering to the details prescribed for each technical division of the project is it possible to conduct these complex operations without hazard of loss of critical data. Comprehensive photographic coverage provides essential positional correlation for the oscillographic data. In addition, these 30 photographic devices record observations not provided by other instrumentation, and therefore, are also primary sources of data.

ANALYSIS AND FINDINGS

Force and Acceleration Data

The intersection collision is among the most complex of collision exposures. This is because of the multivariant conditions that exist. The principal variables requiring

consideration are speed, angle of impact, eccentricities of impact, and the structural properties and weight of the vehicles involved. All these variables were held constant for the correlate collisions presented in this paper for the purposes previously described. Triaxial accelerometers were used to provide resultant acceleration data for the car and occupants.

Figures 4 and 5 show time after impact, in seconds, on the abscissa located to the right of the struck car diagram. The transducer patterns are drawn to scale in correspondence with this time axis and with peak values shown to enable the value of any ordinant position to be computed. In addition, the seated positions of the adult, child, and infant dummies are shown for each car.

Figures 4 and 5 show the striking car for both Experiments 57 and 62 registered a 10G peak acceleration; the struck car for Experiment 57 registered 16G compared with 17G for the struck car of Experiment 62. This close correlation supports the value of

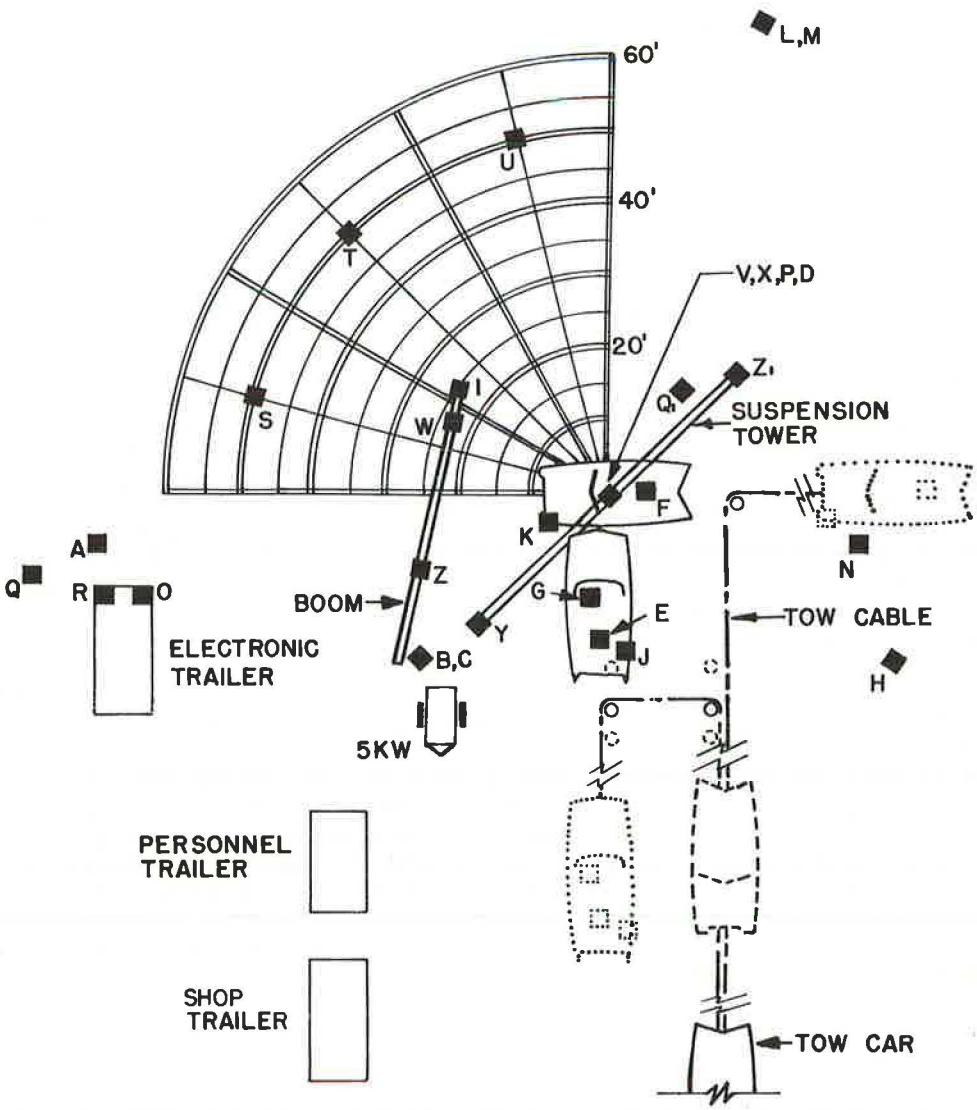

Figure 3. Vehicle control and photographic systems.

TABLE 1

INSTRUMENTATION

Device	Purpose	Location	Specifications
Camera:			
High-speed	Displacement/time for automobile and dummy kinematic data	Cameras A, B, C, and D (Fig. 3)	Eastman I & II and Fastax WF-3, 16-mm Kodak Ektachrome ER 7257, 600-1,000 frames per sec (f/s)
Moderately high-speed	Displacement/time for automobile and dummy kinematic data	Cameras E, F, G, J, K, L, M, N, and O (Fig. 3)	8-Photosonics 1B, Traid, and 1-Urban Engr. Co. GSAP MBH 200-16, high G tolerance 200 f/s, 16-mm Kodak Ektachrome 7257
Standard	General and backup photographic coverage	Cameras P, Q, R, S, T, U, V, and W (Fig. 3)	1-K-200 with 170° lens at 64 f/s; 2 Bolex, Zoom lens at 24 f/s; 4 GSAPS wide angle lens at 64 f/s; 1 Cine Special, 1-in. lens at 64 f/s; all 16-mm Ektachrome 7255
Special	Larger format; sequentials photographs of collision events	Camera H on 20-ft tower. Camera I on 40-ft boom tower (Fig. 3)	Hulcher Model 102, 20 f/s 70-mm Super Anscochrome (Camera rotated 90° to permit cine-reduction) Camera I, Bell & Howell Eyemo, 48 f/s Ektachrome ER 5257; both cameras have rotating shutters
Still	Precision-timed photographs	Cameras X, Y, Z, Z_1 (Fig. 3)	Super Speed Graflex 4 × 5 Ektachrome 1/1,000-sec electronically controlled to fire at precalculated millisec after contact
Calibrated references	A calibrated and fixed reference during impact	Near impact center	¼-by 6-by 96-in. plywood, vertical 4-ft posts and ropes calibrated yellow and black alternate 1-ft increments, positioned both vertically and horizontally
Reference targets	Precision photographic references for micromotion analysis	On points of interest for both car and occupants.	5-by 2-in. diamond-shaped yellow and black targets
Electrical accelerometer	Sensing of acceleration	For both vehicles triaxial accelerometers at right side station-9 frame; driver's and passenger's chests, driver's head	B & F LF 50-50 and LF 50-100; Statham A 38 a-60-350 and AE-100-350
Seat belt tensiometer	Sensing belt loads	Between floor pan anchorage and belt webbing for lap belt and between passenger shoulder and door post anchorage for passenger shoulder belt	See (1) for dual--type strain gage description
Recording oscillograph	Amplitude-time records of transducer signals	Carried by instrument recording vehicle	18-channel Consolidated Electrodynamics oscillograph, type 5-114 P2 with related converter and power supply
Electronic delay timers	Precision timing for still photography	Electric pressure pads near impact center	200- and 500-millisec time delay devices built by ITTE
Photographic oscillographic synchronization unit	Zero time (vehicle contact); flash bulb for film and pulse for oscillograph	Pressure switches between car contacting surfaces and flash bulb photocell on car hoods	See (1)
Pulse generator	Timing for hi-speed cameras	Between camera and power source	Wallensak, 100 and 1,000 cps
Auxiliary timer	Backup timing	Near impact center in view of all cameras	Rotating yellow and black drum; constant-speed 1,740-rpm motor
Wheel revolution counter	Car speed data	Right rear wheel of both vehicles	Induction pickup for oscillograph
Tire-skidmark tracer	Identification of which tires generated skids	On each tire-rib, ¼ in. from road surface	Artist-type oil paint deposits
Deflection recorders	Measurements of differential motion of body and door latch components	Approximately 20 positions on doors and door latches	2½-in. bronze stylus arm bracket on car body, door on latch with stylus spring loaded against carbon-blackened polished chrome or glass plate, secured to adjacent member
Polar coordinate grid	Position data for vehicles from point of impact to positions of rest	On asphalt surface at test site	Yellow traffic marker paint on asphalt (Fig. 3)

carefully controlled collision experiments and establishes that prior collision exposure of a car will not significantly alter its collision performance, provided it has been properly repaired.

Not all the positions monitored by instrumentation in Experiment 57 were exactly repeated in Experiment 62. For example, in Experiment 57 the front seat passenger of the striking car was instrumented for chest acceleration and combination shoulder strap and lap belt load. In Experiment 62, this same dummy was instrumented for lap belt force data only. His triaxial chest transducers were transferred to the three-year-old child standing behind him in order to provide initial acceleration data for children undergoing this type of exposure. A similar repositioning of transducers from the chest of the passenger for the struck car in Experiment 57 was made for Experiment 62 to provide the three-year-old in the struck car with chest transducer instrumentation.

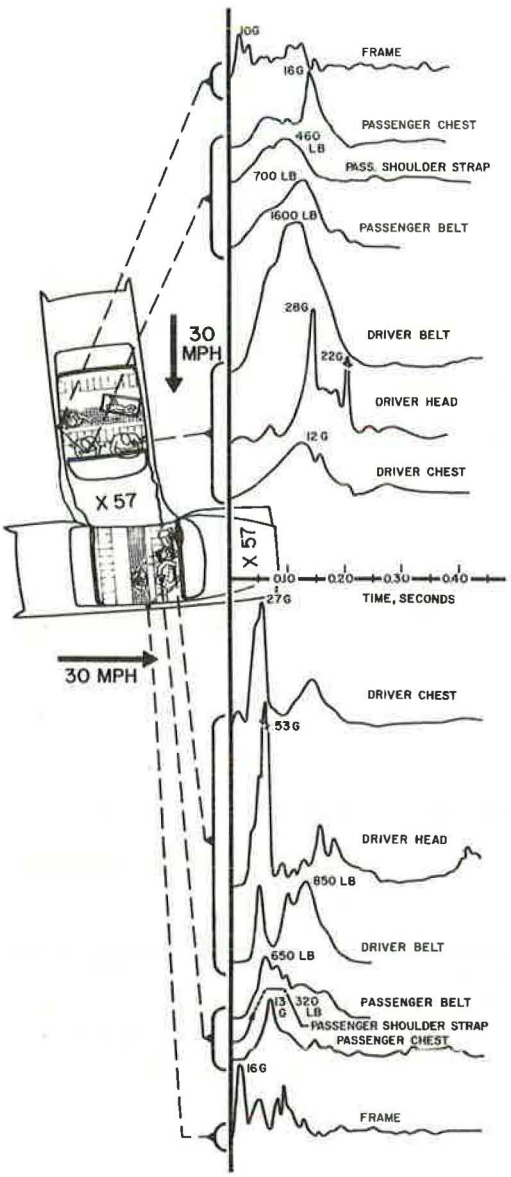

Figure 4. Transducer patterns, X-57, center-side impact, 30 mph.

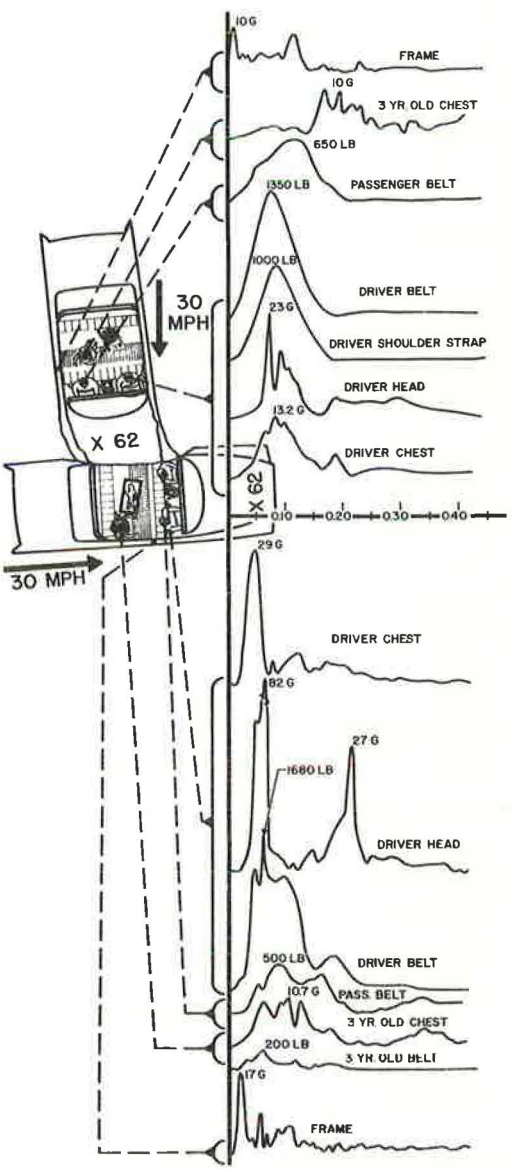

Figure 5. Transducer patterns, X-62, center-side impact, 30 mph.

TABLE 2

ANTHROPOMETRIC DUMMY SPECIFICATIONS

Dummy	Seated Position	Height (in.)	Gross Weight (lb)	Joint Articulation	Manufacturer
Adult drivers[a]	Left front	72	200	Principal	Sierra Engineering Model 157
Adult passengers[a]	Right front	68	170	Principal	Sierra Engineering Models 292 & 185
Children	Rear seat	35	37	Five only[b]	UCLA-ITTE
Infants	Rear seats	26	12	Five only[b]	UCLA-ITTE

[a]Drivers were interchanged from striking to struck car to accommodate use of special head camera installed in one of these driver's heads. Their identical specifications permitted this interchange without introducing any bias. Corresponding passenger dummy was transferred in each instance.

[b]Five joints: arms at shoulder girdle, legs at pelvic girdle, and a single neck joint. Joints have limited action of conventional toy doll. A three-year-old child anthropometric dummy having trauma sensitivity is currently being manufactured to UCLA-ITTE specifications.

Safety belt tensiometer loads, per se, are not particularly significant unless the heights and weights of the restrained anthropometric dummies are likewise provided. Table 2 assists in judging the relative significance of the various belt forces discussed in this paper. The exact meaning of these tensiometer peak load values is not clear without further explanation of what this instrumentation measures. Belt tensiometer data represent the forces at belt anchor points on the car structure. Furthermore, the lap belt tensiometer values represent the total tension on the two anchor points, or loop-load, whereas the passenger shoulder strap tensiometer values represent the tension at the single shoulder anchor point at the center doorpost and is not a measure of the chest loop-load. The lap belt tensiometer peak values may be expected to increase in a rather uniform manner, with respect to increases in impact velocity, because they tend to compensate for the effects of lateral body loading components. This occurs because the tensiometer toward which the body is thrown may show reduced tension whereas the other unit, for this same body displacement, would show a correspondingly increased value.

The passenger shoulder strap tensiometer values should not be regarded as absolute upper torso restraint forces but rather as approximate values having reasonably good correlation with the variables of speed and impact configuration, because of the following interactions:

1. During collision, changes in the motorist inertia force vector as a function of time causes a continuous misalignment, both vertically and horizontally, between the shoulder strap and the direction of the motorist's inertia force.
2. Variability of the strap-to-motorist-body frictional forces are recorded by the tensiometer at the strap anchor point as though they were true restraint force variations.
3. The slip-link feature of the combination belt under study permits shoulder strap anchorage forces to be a function of lap belt forces.

The passenger shoulder strap tensiometer readings are valid only with respect to the tensile force acting at the doorpost anchorage, although they do provide a useful indication of the relative severity of collisions.

Driver Exposures

The driver dummies for all four car exposures were provided with head and chest

triaxial accelerometers and safety belt tensiometer instrumentation. Inasmuch as the car's collision performance remained substantially the same, despite a prior divergent history of collision, driver interaction with the car's interior provided valid comparative data. Furthermore, to obtain greater usefulness from this correlate experiment, it was desirable to evaluate additional dependent variables. The restraining devices for the front-seat adult dummies of the striking car were interchanged. In Experiment 57 the driver of the striking car wore a lap belt only, whereas in X-62 this same driver wore a combination shoulder strap and lap belt. The driver's head deceleration resulting from his head striking the steering wheel in X-57 registered 28G, in contrast with 23G for X-62. The added restraint of the shoulder strap in X-62 accounted for the reduced head acceleration. The driver stressed this shoulder strap to a registered 1,000 lb during the impact, while his lap belt simultaneously reached a peak of 1,350 lb. A slip-link feature of this combination belt provides for automatic adjustment during impact for variations in chest and hip restraint force magnitudes.

Driver Dummy Interaction with Tempered and Laminated Side Glass

The resistance of safety glass to breakage depends on a variety of factors, identified by another paper (3). A brief review of these factors will assist in understanding the findings to follow. The stresses applied to glass during impact depend on the mass, contact geometry, velocity, and resilience of the impacting object as well as on the type and thickness of glass, ambient temperature, glass edge constraint, and other physical factors of this nature. When the impacting object is a human head, a difficult problem arises when attempting to select impact performance specifications for safety glass that will provide uniform rather than selective protection from injury. As the strength of glass—either tempered or laminated—is increased it tends to reduce the frequency of breakage, thus improving occupant protection from being ejected, protection from roof collapse during upset and perhaps most important, to reduce exposure to laceration. However, as the strength of glass increases, so does the frequency of brain concussions and skull fractures.

Although subject to several qualifications to follow, briefly stated, laminated glass as used in automobiles has a relatively high resistance to impact by small, sharp objects, whereas tempered glass has a relatively high resistance to impact by blunt objects. The following qualifications are appropriate to this statement:

1. The statement is true if resistance to impact means resistance to glass fracture. Laminated glass may fracture with the appearance of a single localized crack, or with a simple pattern of several cracks or it may fracture with total breakage accompanied with varying amounts of fragment dispersal. Tempered glass fracture extends almost instantaneously throughout the entire sheet and is generally accompanied by a complete dispersal of glass fragment.
2. The resistance that tempered glass exerts against a striking object terminates on fracturing. For laminated glass, this resistance continues to function following fracture until the plastic interlayer is ruptured.
3. Resistance to impact by tempered and laminated safety glass is a function of changes in glass continuity induced by the impact. For one range of impacts, laminated glass would be cracked substantially but tempered glass would be unbroken. For another range of impacts, laminated glass, although cracked and possibly punctured, would still function as a more or less cohesive surface but the tempered glass would be completely shattered out. And for still another range of impacts, both types of glass would be entirely or mostly broken out, although not necessarily with the same degree of hazard.
4. Resistance to impact by glass is a function of thickness and whenever comparisons between tempered and laminated glass are being made in this paper, their respective thicknesses may be assumed equal unless specified otherwise. Accordingly, resistance to impact may carry different interpretations, depending on the nature of the impact and the type of glass. With respect to nature of impact, the UCLA-ITTE project determined three causes for side-window breakage during intersection collisions:

   (a) Abrupt lateral acceleration of the window frame and glass into the motorist's head;

(b) Comparable action into the motorist's shoulder by the window sill, sufficient to break window glass; and
(c) Encroachment by the striking car into the struck car side below its window level, or direct contact with its window.

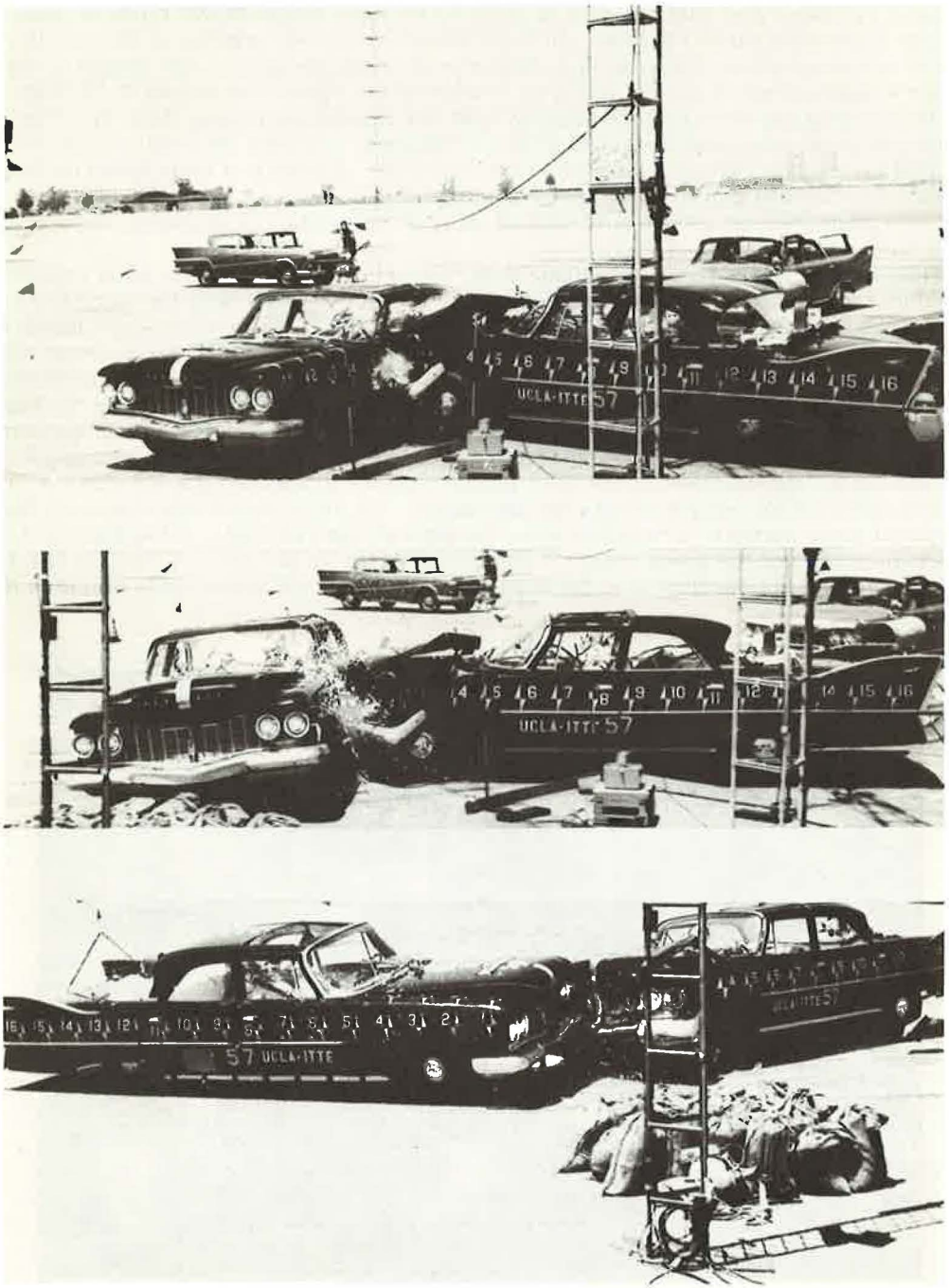

Figure 6. Experiment 57.

The correlate Experiments 57 and 62 demonstrated the head impact action described by item 1, accompanied to some extent by the interaction described by 2. With respect to item 3, inasmuch as the striking car impacted the driver's door, this mechanism for side-window glass fracture also operated, but as will be shown, with varying influence on the struck car driver's head blow—according to whether tempered or laminated glass was installed. Concerning item 4, the nominal thickness of the glass was $\frac{1}{4}$ in.

The driver of the struck car for both X-57 and X-62 wore a lap belt only. This condition of restraint was held constant in order to evaluate two different types of side-window glass adjacent to his head. In X-57 the left front side-window of the struck car was of tempered glass, whereas in X-62 it was of laminated glass. The impact of the driver's head shattered out the left front window of the struck car during X-57 (Fig. 6): the laminated glass was fractured during X-62 but remained in place (Fig. 7). The tempered glass accounted for a 53G peak acceleration, whereas the laminated glass accounted for an 82G peak acceleration (Figs. 4 and 5). Analysis of high-speed motion picture film showed that in both instances the head struck the side-window glass and that this glass was not additionally backed up by direct contact of opposing striking car structure.

The explanation for these anomalous data, wherein the resistance to blunt impact by tempered glass was less than the resistance by laminated glass of the same thickness, may be found by referring to the three causes of side-window breakage mentioned earlier. Inasmuch as both heads were seen by high-speed photography impacting the side glass, this action was quite understandably assumed to be the cause of the glass fracture. However, the other two factors, the motorist's shoulder stressing the base of the window and the striking car encroachment below the window were also operating and with considerable force. It appears that these stress concentrations increased sufficiently during the onset of the head impact with the glass to crack the glass with results different for tempered than for laminated. All head impact resistance by the tempered glass abruptly terminated when the edge stress reached a value sufficient to crack the glass and the glass ruptured completely from its mounts. A similar crack or series of cracks developing in the laminated glass will not appreciably diminish its

Figure 7. Experiment 62.

resistance to head impact because the cohesive properties of the plastic interlayer continue to function following initial cracking.

This explanation is supported independently by laboratory studies conducted at UCLA by the ITTE collision research project in which identical 1960 Plymouth doors were mounted with the same door hinge and latch restraints and their side glass impacted with a 9-lb simulated human head. Under these controlled conditions, and without the edge stress concentrations identified with full-scale collision studies, the impact velocity that produced a peak acceleration of 83G for laminated glass produced a peak acceleration of 130G for tempered glass of the same thickness.

These laboratory studies were conducted using a mass and impact velocity, for the simulated human head, comparable to the anthropometric dummy head mass and velocity, in which the side window was accelerated to impact the dummy's head during the full-scale collision experiments. The poor correlation between head impacts of 53G, for the full-scale crash, and 130G for the laboratory study, provides additional data indicating the sensitivity of tempered glass to coincidental edge stressing during collision. This observation is strengthened by the fact that high edge stressing was positively identified as accompanying head impact during the full-scale collisions and the laboratory studies were controlled to exclude edge stressing during head impact.

Additionally, the close correlation between the head impact peak acceleration of 82G obtained by full-scale crash tests and the head impact of 83G obtained by laboratory tests demonstrated the relative insensitivity of laminated glass to coincidental edge stressing during impact.

Driver Lap Belt Forces

The driver's chest for the struck car of X-57 and 62 registered 27 and 29G, respectively. The drivers of the struck car, X-57 and X-62, wore lap belts only. Poor driver seat belt correlation was obtained considering an 850-lb force was recorded for the driver of X-57 as compared with 1,680 lb for the driver in X-62. The explanation for this gross deviation may be found in an earlier publication (2) which states that seat belt force for this exposure is not a realistic source of data. The driver is pinned against the side of the car because of the abrupt acceleration the car received from the striking car; to the extent that the driver's belt in Experiment 57 was not as snug as it was in Experiment 62, the reading would be correspondingly less because a very slight translation by the driver's hips to his left will be abruptly checked by the intrusion of the striking car. Additionally, the intrusion of the striking car may produce seat belt displacements in the direction of advance of the striking car that are being recorded but have little bearing on real inertial forces of the dummy. Finally, the striking car in X-62 may have developed direct mechanical interaction with the tensiometer, one of which was located where the striking car intrusion was greatest.

Adult Dummy Restraint

Strong transverse forces are applied to motorists during intersection collisions. The purpose of including the combination shoulder and lap belt restraint configuration in the Series II intersection collision experiments was to provide an evaluation of the possible added advantage of a diagonal chest strap in reducing upper torso movement during impact. As reported in a prior publication covering 12 intersection collision experiments (2), the combination chest and lap strap provided effective restraint from these transverse forces in the majority of exposures. For the correlate Experiment 62, the diagonal chest strap of the front seat passenger of the struck car was eliminated so that this exposure could be studied for a dummy during collision wearing a lap belt only. Figure 4 shows the combination belt for the front seat passenger, struck car, registered 650-lb lap load and 320-lb shoulder belt load. This may be compared with the 500 lb for the lap belt load for the identical exposure in Experiment 62, wherein the dummy wore only a lap belt (Fig. 5). In X-57, one of the two lap belt anchorages is also the anchorage for the shoulder strap. Its tensiometer, therefore, records part of the chest strap load. In addition, examination of high-speed motion picture film provided additional information. Under the comparable collision conditions of Experi-

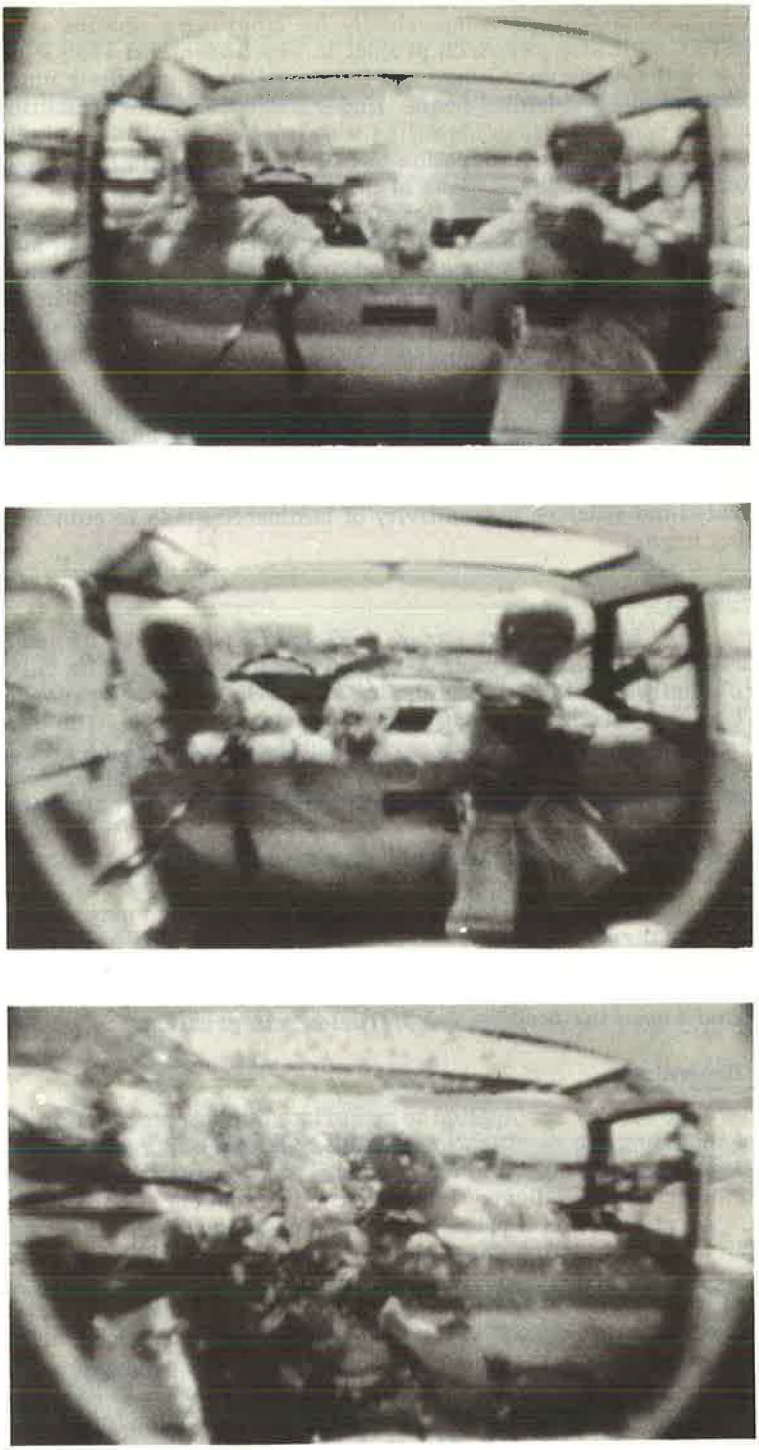

Figure 8. Inside struck car, X-57.

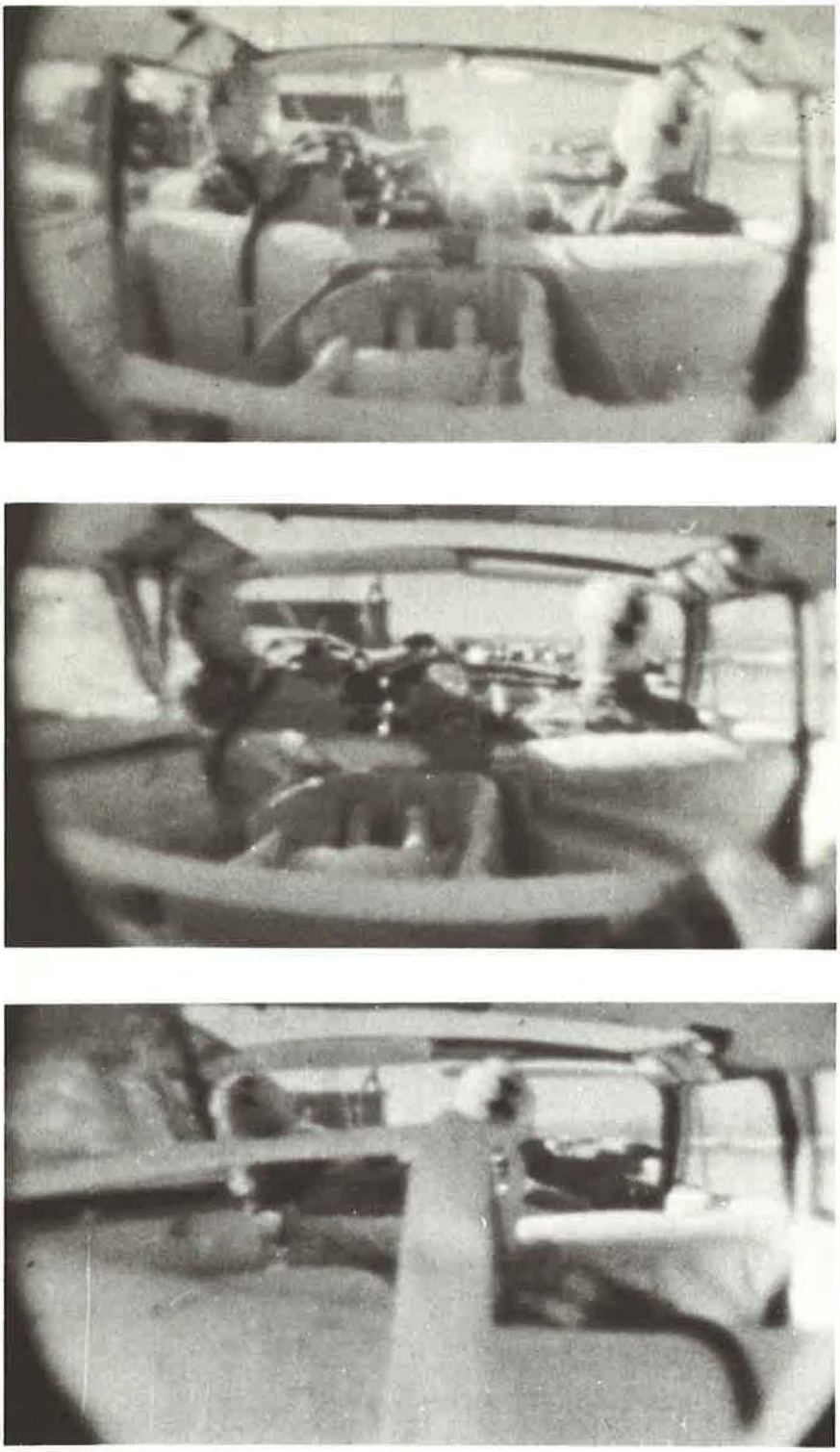

Figure 9. Inside struck car, X-62.

ment 62, the upper torso was permitted a greater lateral movement sufficient to strike the occupant seated to this dummy's left and this form of upper torso "restraint" is not presented as an added lap belt loading.

This discussion has concerned the movement of the right front seat passenger of the struck car illustrated in the sequence Figure 8 (X-57) and the companion Figure 9 (X-62). The shoulder cross-strap shown in Figure 8 for the front seat passenger passes from upper right shoulder to lower left hip and, therefore, does not offer as positive an upper torso restraint for impacts directed to the left side of the car, as for impacts directed at the right side. To the extent that the struck car is moving forward when impacted at its side, the contact at the side by the striking car decelerates the struck car; the inertial forces of the right front seat passenger develop forward movement of the dummy's hips (relative to the car interior) that function to tighten, through the slip-link, the diagonal chest strap. As a consequence of this slip-link feature, in the majority of the UCLA intersection collisions directed toward the belt side affording reduced protection, the dummy appeared to be rather well restrained by the cross-strap during the collision. The right front seat occupant's sideward movement for the two 30-mph correlate experiments shown in Figures 8 and 9 (struck car) was approximately the same for the dummy with a diagonal strap and lap belt as for the dummy with only the lap belt. Some allowance should be made, however, for the reduced degree of spinal articulation common to anthropometric dummies, as compared with their human counterpart.

In X-62, this right front seat passenger would subsequently have been ejected had he not been wearing a lap belt (Fig. 10). Under this same exposure condition a human might have had his head and shoulders partially ejected even though wearing a lap belt, and this is hazardous particularly if the car subsequently overturned or struck another object. The shoulder cross-strap is useful in reducing this tendency for the upper torso to be thrown outside an open door. The installation shown in Figure 8 is higher than shoulder height. It was found that severe neck lacerations can result when this strap functions to restrain upper torso ejection with the upper anchorage point substantially above shoulder height. Accordingly, the upper anchorage point for this strap should not be above shoulder height.

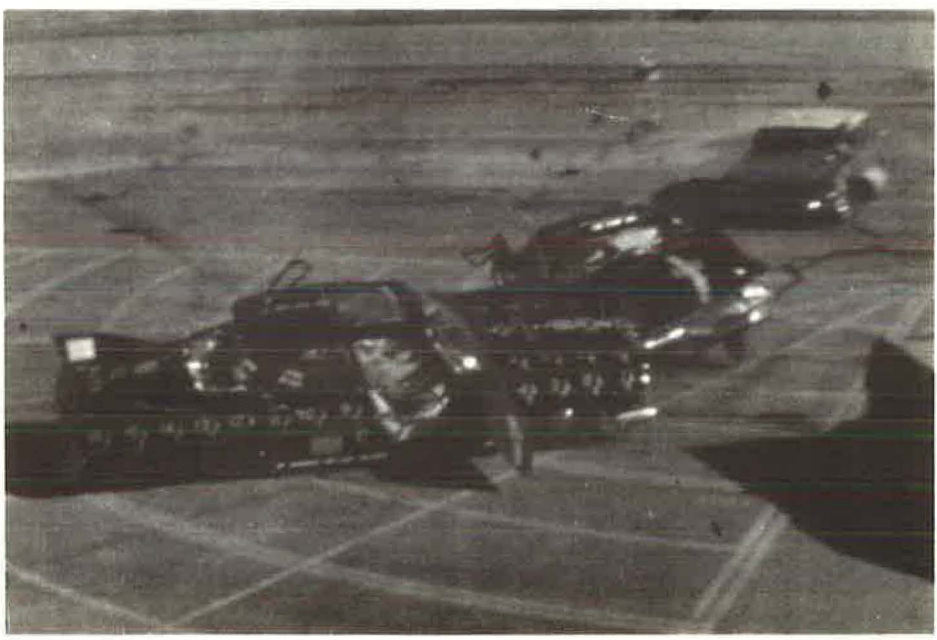

Figure 10. Door latch failure.

Child Motorist

Simulated children were included in this correlate experiment to provide additional information on the relative exposure hazards of children in various seated positions and postures with various means of restraints. In Experiment 62 the instrumented three-year-olds registered a 10G chest deceleration when riding in the striking car and a 10.7G chest deceleration when riding in the struck car (Fig. 5). However, the three-year-old in the struck car is secured by a lap belt that registered 200-lb loading, whereas the three-year-old in the striking car was unrestrained. The exposure positions are generally more severe for occupants in the struck car. The unrestrained child that was subjected to a 10G peak chest deceleration will frequently receive serious head injuries, for this exposure. The Figure 8 sequence, X-57, shows the probable extreme abuse a child experiences during impact when standing behind the front seat in the struck car. Under identical collision exposure conditions for X-62, except with this child dummy sitting on a cushion and restrained by an adult-type lap belt, the child was observed riding out the impact in an uneventful manner.

In the same Experiment 62, referring this time to the striking car, a similar three-year-old child dummy was equally as effectively protected by the adult-type lap belt; although the rear seat back tore loose and contributed to the forces the dummy sustained (Fig. 11). When the three-year-old is standing on the right side, behind the front seat in the striking car, the exposure is substantially less than the comparable position for the struck car, because the striking car is abruptly jerked to its left, tending to pin the child against the right side of the car in a not-too-abusive manner. This description assumes that the right rear door remains closed under the high-collision tension-failure forces that are augmented by human body inertia forces collectively acting to open the door. Had the struck car been traveling in the opposite direction, the child would have been thrown violently across the front seat back to her left much in the manner experienced by the child shown in the Figure 8 sequence.

Infant Motorists

Six-month-old simulated infants were included in these correlate experiments, one to each car. In the prior series of 12 intersection collisions, it was found that a bassinet whose long axis paralleled the long axis of the car, positioned behind the center of the front seat back and appropriately anchored, provided the best location. In Experiment 62, this location was repeated and the findings confirmed these prior observations. Of special interest, X-62 emphasized the importance of providing a protective covering (such as a net) for the bassinet. The bassinet anchorage held but the bassinet was forced substantially to the left as a result of the impact at the left side of the car. Impact forces were sufficient to throw the simulated infant from her bassinet. The three-year-old sitting in the rear seat to the right of the bassinet was restrained by a lap belt and, therefore, did not interact adversely with the bassinet as had been observed in prior collision experiments where the three-year-old was not restrained.

The infant standing in the center of the front seat of this struck car was provided with harness-type restraint and may be seen in Figure 9 riding out the crash in a rather uneventful manner, except for the abusive force applied subsequently by the adult sitting to her right (Fig. 12). An identical simulated six-month-old with the same harness restraint was seated between the two front seat motorists of the striking car and was observed equally as effectively restrained and was not so severely contacted by these front seat motorists.

The harness worn by these infants demonstrated the value of a well-designed protective restraint. This harness has been commercially available for several years and consists of straps that restrain the chest and shoulders interconnected with straps that restrain the hips and pelvis. The harness is restrained by a vertically positioned attachment strap that loops the entire car seat back and is anchored to the car floor below and to the rear of the attachment strap. This anchorage of the attachment strap limits forward movement of the seat unit and transmits the infant restraint forces to the car floor pan. A slip-loop feature permits the infant to stand, sit, or lie down on the seat. Even with this freedom of movement, the infant remains effectively restrained against collision forces acting in practically any direction.

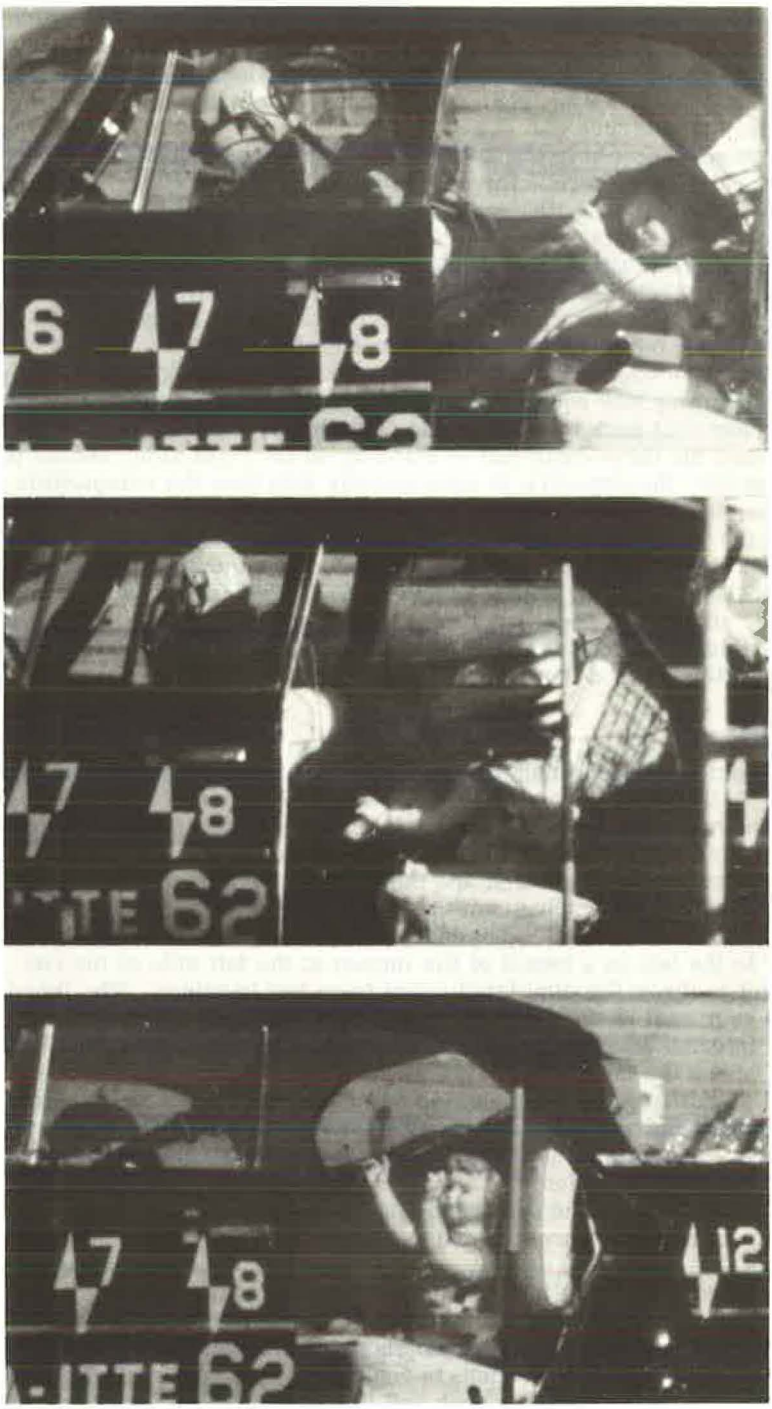

Figure 11. Lap belt protecting 3-yr-old.

Safety belts that transmit forces primarily to the viscera or adjacent areas of the body midway between the pelvic and shoulder girdles are unacceptable as motorist restraints. Manufacture of such devices should not be permitted because they increase rather than diminish the chances of injury during collision by directing collision forces to the more vulnerable portions of the body, a feature diammetrically opposed to the basic principle of protective restraining devices. Although these deficiencies are obvious, such devices are still being manufactured and sold to the public.

In X-57 (struck car) this same front seat center position for the infant was evaluated by having her seated in a bail-type car seat. A detailed discussion of this unsatisfactory seat performance during impact may be found elsewhere (2). Briefly, it was found that the bail fasteners readily detach during impact, permitting seat and child to strike the car interior. Should the bails not detach, adverse forces are applied by the chrome tubing to the infant's viscera. The infant for this seated position is exposed to the crushing forces of adult front seat motorists unavoidably thrown against the infant during impact. The rear seat, center position, is safest seat position for infants and children. Protective restraints can be applied for this seat position that do not restrict the child's need for some freedom of movement and that additionally permit the child to see the passing view outside the car. The driver remains undisturbed from his important task and the child is restrained in the position of greatest protection from collision forces, regardless of direction. From these preliminary findings, therefore, the harness restraint as previously described permitting the infant to stand or lie down is a satisfactory restraint and is the safest of infant restraint systems evaluated to date.

The striking car rear seat, for X-57, carried a bassinet resting on the seat. During impact the rather high acceleration forces to the striking car's left threw the bassinet from the seat to its right; however, the infant remained within the semi-protective confines of the bassinet. The tie down straps furnished with most bassinets, when properly anchored, greatly increase infant protection during collision.

Figure 12. Impact forcing door open.

Belt Elongation

Instrumentation was applied to all restraining harnesses used in Experiment 62 for the purpose of measuring safety belt fabric permanent set, or elongation. Measurements were recorded to the nearest $\frac{1}{16}$ in. and no permanent set was observed for these collision exposures. This observation can be explained by referring to Figure 4. The forces applied to the safety restraints did not approach the loop strength limits prescribed for these belts. Further, the restraining

webbing used in these automobile collision experiments was about one-half the strength specified for webbing in military aircraft. Even so, the forces it sustained were not sufficient to develop measurable elongation. Furthermore, a comparison of the motorist acceleration exposure levels for the 30-mph correlate experiments with those substantially higher levels established by Stapp, et al., as survivable, leads to the following conclusion: properly restrained, the 30-mph intersection collision is a survivable crash, except possibly for motorists sitting next to the impacted side of the struck car. This statement is not in any way intended to suggest that the 30-mph intersection collision is not a serious accident, but rather to assert that even considering the severity, these crashes are survivable for motorists wearing properly designed, installed, and applied safety belts.

Transducer Data Process

Using manual procedures, data reduction of a single collision experiment, instrumented in the comprehensive manner depicted by this paper, would require one full year of an engineer's time. Each successive experiment tends to be more thoroughly instrumented thereby increasing the data reduction task. To reduce the time required, an attempt was made to take advantage of high-speed computer processes. Previous attempts at UCLA had been unsuccessful because a program able to assimilate correctly the input data of the irregularly shaped curves recorded from transducers during collision had not been devised. A new approach to this problem by highly qualified specialists in computer programing at ITTE-UCLA provided a successful breakthrough. This technique is described in detail elsewhere (2) and is briefly summarized here.

Because of the asymmetrical nature of the intersection collision, impact-acceleration forces may occur in any direction. Bi-directional accelerometers were placed in clusters of three along mutually perpendicular axes to provide X, Y, Z axes sensing positive and negative accelerations. The resultant acceleration values were calculated by the IBM 7090 computer from acceleration values taken at selected common times. In addition to these resultant acceleration values, the directions of these resultants were also indicated; these acceleration vectors referred to the positions that the component transducers occupied, relative to the anthropometric dummy or car structure to which they were attached. The actual orientation of a given cluster of accelerometers at a specific instant during an impact could be determined by reference to one or more of the high-speed motion picture films, synchronized with the transducer data.

The transducers positioned within the car and within dummies were connected by a 100-ft multi-conductor cable to an 18-channel oscillograph carried by the instrument recording car that followed the crash car to the impact area. A flash bulb mounted on the crash car provided a visual signal as well as an electrical pulse indicating zero time for the motion picture and recording oscillograph systems. Appropriate sensitivity calibrations of transducers were made just before and immediately following the collision experiment.

Each oscillograph curve was traced on a separate sheet of vellum to permit inclusion of calibration time lines, scale factors, critical point notations, and other data that would tend to deface the original oscillograph record. The process of extracting the square root of the sum of the squares for the many triaxial data points, of applying the various channel scaling factors and of regraphing to a common scale, was a laborious task quite appropriate for the digital computer. The points to be plotted by the computer were indicated by pencil notation on the vellum graph. These points were spaced irregularly to avoid excluding peaks. This procedure enabled input data to be transferred in a perfunctory manner without loss to final accuracy. A Benson-Lehner "Oscar" curve-reading machine was used to translate the indicated points from the vellum curve onto punched cards. Special techniques were used to correct for deficiencies that are inherent with this machine. For example, each curve was read once by two separate "Oscar" operators who independently prepared punched cards for each transducer curve. Both sets of cards were compared and if found to be in reasonable agreement, both sets were used by the computer. The program provided for the following computer output:

1. A print-out of each curve in tabular and graphical form;

2. Similar print-outs of accelerometer resultants;
3. A print-out of the input data for control purposes; and
4. Information about the accuracy of each computation.

The program that was developed used a sequence of overlapping parabolic curves for computer presentation of the accelerometer durve. This procedure enabled the computer faithfully to follow the sharp peaks occurring at irregularly spaced intervals that are characteristic of accelerometer patterns generated during collisions. Correlation checks were made at all distinct phases of the entire data process as well as by independent techniques, such as comparing computer curves with those produced by hand solutions. Excellent correlation was obtained (2).

COLLISION PERFORMANCE

Vehicle Collision Dynamics

As would be expected, the two cars for these correlate experiments followed approximately the same collision sequence of events, generating about the same car-to-car deformations, approximately the same changes in directions and spin-out patterns as well as reaching about the same positions of rest. These observations are in part identifiable in Figures 6 and 10 for X-57 and 62, respectively.

The simulated motorists inside these cars appeared to respond the same for the two experiments, except for the variations imposed by different types of safety restraints and by the changes in the type of side-window glass they struck. That is, the primary movements of the dummies during collision, as viewed by high-speed photography, closely correlated for corresponding seating positions of X-57 and X-62. However, the type of interior surface encountered (for example, laminated vs tempered side glass) made a difference in dummy transducer readings.

Differences in collision dynamics for X-57 and X-62 may be observed by comparing Figures 13 and 14. Minor variations in corresponding car movements are evident and these differences are more apparent by comparing positions of rest for striking and struck cars.

The changes in direction and the displacements that the cars underwent as they collided and spun out to their positions of rest (Figs. 13 and 14) are given in Table 3.

Figures 15 and 16 provide further opportunity to determine the differences in positions of rest and also indicate the corresponding skid patterns leading to these positions of rest for Experiments 57 and 62. For the Series II intersection collision experiments the crash car brakes were not applied at impact; following impact, brakes were applied only in those instances where a crash car was heading for a tower anchorage or the car moved about 100 ft from the position of impact. No crash car emergency braking was required for X-57 or X-62; the skid patterns shown in Figures 15 and 16 are the result of the collision forces changing car headings. These skid marks may be termed "deviation" skids in those instances where abrupt changes in direction are evident at and next to the position of impact as a direct result of collision forces; "brush" and "centrifugal" skids where such marks are generated by the arcing or spinning car after leaving the position of impact as a secondary result of collision forces. Brush and centrifugal tire-skid marks can be laid down by vehicles attempting turning maneuvers at driving speeds higher than normal for the maneuver but deviation skid marks require a collision for their generation. Deviation skid marks are useful, therefore, in identifying the vehicle position on the roadway at the time of impact. In addition to deviation skid marks, car rim flanges, undersides of bumpers, or fractured bumper supports, and underbody sill metal or frames occasionally are forced into the pavement leaving gouge marks. Correlation of these pavement gouges with abraded metal components found on the wrecked vehicle often provide an objective basis for establishing the position of the car when those pavement gouges were generated. Pavement gouges may be made by the damaged vehicle at the position of impact or on its way to its position of rest, or both. A deviation skid mark is made only during collision: (a) as a result of the tire being abruptly stopped or nearly stopped by intruding structure of the opposing vehicle as the wheel is crushed rearward and frequently sideways, or (b) as a result of

TABLE 3

POLAR DISPLACEMENTS OF CAR CENTER OF MASS FOR 30-MPH CENTER SIDE IMPACT

Experiment	Polar Displacement			
	Striking Car		Struck Car	
	Deg	Ft	Deg	Ft
57	23	33	24	39
62	34	28	31	42

a side impact when the brakes have been previously locked up. The deviation rubber mark on the pavement is blackest when the distressed tire has been overridden by the other colliding vehicle because this places additional load on that tire. In such instances, the deviation skid may also be referred to as a distressed skid mark.

The high load carrying tires (those on the outside of the turn or spin) generate brush skids and their patterns for corresponding wheels of X-57 and X-62 followed the same general positioning relative to the impact axes; three corresponding skid patterns coincided within 1 ft of each other and the remaining two sets of patterns differed by an amount not exceeding $2\frac{1}{2}$ ft.

Non-braked brush skids are generated by tires on the advancing side of the arc that the center of mass of the car is following. This statement allows for the fact that, as a car spins out along a given trajectory, tires on the right or left side may alternately mark and then not mark the pavement according to whether they are on the advancing side of the arc or on the trailing side of the arc, respectively. The tires on the trailing side may carry a car load insufficient to generate observable rubber brush marks on the pavement. At times, these tires are entirely off the pavement (Fig. 6).

In X-62, the striking car rolled backwards 2 ft after it stopped broadside skidding. This caused the position of rest to be offset slightly from the terminal positions of skids. The dispersal of collision debris covered approximately the same area for both experiments and these data were presented for X-57 elsewhere (2, Fig. 8).

Coefficients of Friction During Post-Contact Spin-Out Trajectories

On approaching a curve in the road, a driver turns his steering wheel to establish a front wheel deflection that builds up the yawing velocity to a steady state (for constant car speed and constant road radius of curvature, superelevation, and coefficient of friction). (There is a significant lapse-distance between the point where steering wheel turning is initiated and the point where the car body starts to track the turn. As an example, at 35 mph this may be 30 ft and will vary depending on such factors as highway and vehicle design.) If the radius of curvature is too small (that is, the curve is too sharp for the car's approach speed), the minimum radius of turn the car can negotiate for that speed will exceed the geographic radius of curvature of the road; in a sustained curve, the car will drift lanes and leave the pavement. Any attempt to counteract this plight by turning the steering wheel to a larger front wheel deflection will disrupt the steady state yawing velocity and, thereafter, the yawing velocity will continue to increase as the car spins out of its turn.

It is generally conceded that tire-to-road side force during a turning maneuver may approach the value attainable for car deceleration by impending or locked-wheel skids in a straight forward direction. This judgment is based on the assumption that the transverse resistance the road surface offers to tire side-slip is about the same as the linear resistance the tire encounters for braked skid conditions in a forward direction; the calculated values of both resistive forces of friction are based on the same laws of motion and friction. Implicit in this judgment is the assumption, however, that only the tire is in contact with the road surface and does not include the more extreme con-

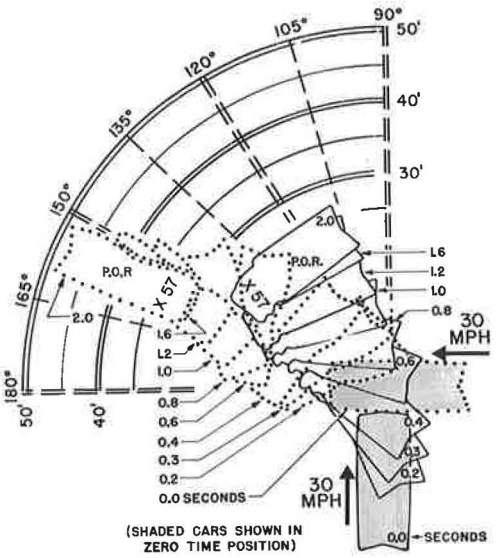

Figure 13. Collision dynamics, X-57, center-side impact, 30 mph.

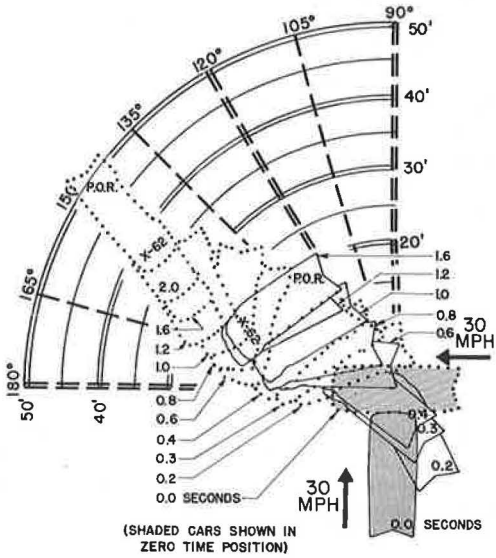

Figure 14. Collision dynamics, X-62, center-side impact, 30 mph.

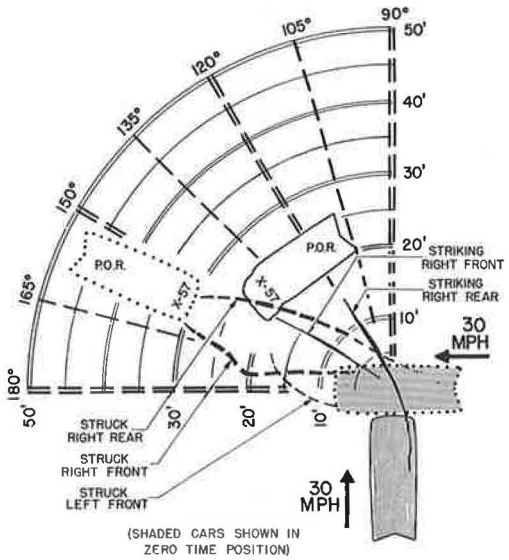

Figure 15. Position of impact, skid marks, and positions of rest, X-57.

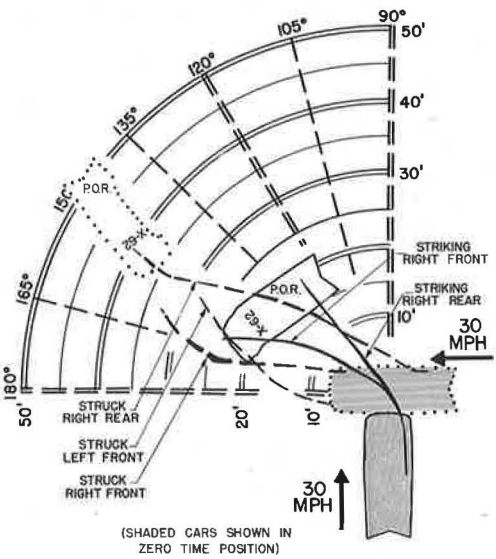

Figure 16. Position of impact, skid marks, and positions of rest, X-62.

ditions that bring into road contact not only the tire but also its rim and at times the car's sill. Also implicit is the assumption that the tire and wheel suspension dynamics provide as effective a tire-to-road gripping continuity for side-slip action as for straight ahead wheel skid action. The motions of a skidding automobile are treated rather comprehensively by Radt and Milliken (4).

Calculations were made to estimate the effective coefficient of friction for a colliding car undergoing post-contact spin-out starting with the instant the car broke contact with the opposing car and continuing to the car's position of rest. These coefficients of friction were calculated for a uniform, level, clean and dry asphalt surface that had a four-wheel locked skid coefficient of friction over the same speed range of 0.75. However, before mentioning findings, a further discussion of principal variables operating during spin-out will assist with an interpretation of data.

As the two cars contact each other during an intersection collision, each car's direction is modified so that it has a new heading and trajectory by the time contact is broken. The heading, or direction the car is pointing at any instant after contact may or may not be the same as the trajectory or direction the car is moving. In a broad-skid, the car is heading at a right angle to the direction it is moving. If the car spins out from impact to its position of rest, it may pass through both a broad-skid, or full brush-skid heading, and subsequently through a no brush-skid heading as it moves towards its position of rest. When the car is in a broad-side skid the effective coefficient of friction may exceed the locked wheel skid coefficient of friction. This will depend, however, on the extent of rim-gouging, which may occur even though the tires remain fully inflated, and also whether the car body-sill contacts the pavement.

Such car-metal-to-road contact will generate sparks and occasionally pavement scrape marks will be visible following the collision. This contact more often is evident, however, not by studying the road surface for scrapes but by inspecting the car rim flanges and body-sill areas for pavement abrasions. During spin-out, as the car's heading comes into alignment with the direction (or the reverse direction) the car is moving, the effective coefficient of friction diminishes substantially. Crippled wheel suspension, collapsed frame structure, or driver braking may singularly or in combination act to prevent this coefficient from approaching zero.

In some of the Series II intersection collisions, the car spun and then rolled on its wheels an additional distance before coming to rest. In others, the car started a spin at impact approaching a broadside skid as it came to rest. Cars in a third group had their headings altered by impact but continued thereafter to roll towards their positions of rest. Speed at impact, position of impact, and to a lesser extent, the respective types of cars involved are the principal independent variables operating to modify collision dynamics.

(The Series II cars were 1960 vintage and their low center of gravity and wide tread prevented upset. Cars of 1950 vintage were used in the Series I experiments and for an impact configuration, identical to X-57, and X-62, both striking and struck cars were overturned. However, corresponding positions of rest were similar, even though the older cars had undergone collision upset en route to their positions of rest.)

Examples of specific values of average effective coefficients of friction (f) for cars primarily undergoing broadside skidding are f = 0.7 for the struck car of X-57; f = 0.6 for the struck car of X-58; f = 0.9 for the striking car of X-61.

Damage Patterns and Costs to Repair

For the same make, model, and year car involved in the same type of 30-mph intersection collision on two occasions (X-57 and X-62), it is not surprising that the same damage patterns were produced for the striking cars and the struck cars of these experiments. That is to say that the location, extent, and nature of damage for these corresponding cars did not provide differences identifiable subjectively. To measure the amount the striking car crushed into the struck car during impact, a frame of reference for each of these cars had to be selected that was not also undergoing observable distortion. The high-speed motion picture films obtained from tower cameras provided the data; preliminary analysis of these films led to the selection of the windshield base

chrome trim as reference for the striking car and the right side door horizontal chrome trim as position reference for the struck car.

Maximum mutual compression is a measure of the change in distance from collision contact to maximum intrusion for the striking car's windshield as it crushes towards the non-impacted side of the struck car. In Experiment 57, this amounted to 1.9 ft; for X-62, 2.0 ft. Minor differences in intrusion for the struck car of X-62 may be explained as follows: in Experiment 61, the struck car had sustained damage that required section welding of the sill below the left side doorpost to prepare it for use in Experiment 62. Forces generated in X-62 were sufficient to break both the doorpost-to-sill weld and the rocker-section weld. Slightly greater intrusion by the striking car into the rear passenger compartment resulted for X-62 as contrasted with its correlate Experiment 57. Where section welding is required to repair a damaged vehicle, these welded sections should be strengthened or helium arc-welded to restore the original passenger compartment integrity. The collision damage sustained by cars provides a good indication of the relative speeds of the cars at the instant of impact. However, impact damage must be considered with respect to other factors such as the relative weights of the cars, their impact configuration, secondary or tertiary collisions, and the like. Controlled collision experiments provide data on impact speed vs cost of repairs and maximum collapse distances.

With respect to cost of repairs, the averages of three estimates received for the X-57 and X-62 striking cars were $710 and $670, respectively, and for the X-57 and X-62 struck cars, $830 and $970, respectively. The slightly greater intrusion for X-62 was reflected in significantly higher repair estimates.

Car Collision Forces

Accelerometer patterns are characterized by their rates of onset, peak accelerations and duration of acceleration at any given level. The relative severity of collisions for corresponding accident types may be established by comparing the peak accelerations attained by intact or noncollapsed portions of the motorist's compartment. Referring to Experiment 57, the striking car, traveling 30 mph at impact, reached a peak acceleration of 10G and this corresponded exactly with the peak acceleration obtained by the 30-mph striking car in Experiment 62. (Acceleration means the striking car decelerates on contacting the side of the struck car but is simultaneously accelerated in the direction the struck car was moving at impact. Triaxial transducers provide the resultant acceleration which reached, in this instant, a peak value of 10G.) The acceleration-time patterns are not identical but their basic characteristics of rate of onset, peak G, and duration show close correspondence. This condition indicates that the motorists in the striking cars were subjected to practically the same collision environment for these correlate exposures. Comparison of the struck cars' peak acceleration shows close correspondence, 16G for X-57 and 17G for X-62. The collision environments for the two struck cars were therefore, essentially the same. This observation takes on added importance when making comparisons between the performance effectiveness for the different restraint configurations worn for X-57 and X-62, as discussed earlier.

Laminated and Tempered Side-Window Glass

For Experiment 57 the struck car side-window glass was tempered and both left rear and left front windows were shattered with greater than 50 percent of the glass dispersal forced inside the car (Fig. 8). For Experiment 62 under the same collision exposure conditions, laminated side-window glass was installed. Both front and rear side-window glass fractured extensively but remained in place, except for about 10 percent of the glass for the upper forward corner of the left rear window that dislodged and was found inside the rear seat compartment.

The high-speed camera mounted on the hat shelf of the struck car, X-62, showed that this small section of laminated glass broke into several smaller pieces as it was projected into the passenger compartment. These fragments were too few to be conspicuous in the individual motion picture frames (Fig. 9), but are observable when

viewing the actual motion pictures. In contrast, a dense shower of fast-moving glass particles from the left front and left rear side-window glass penetrated the passenger compartment during the correlate collision X-57. The only difference for these two exposures was that tempered side glass was installed for X-57 and laminated glass for X-62.

With respect to the tempered side-window glass failures, it was found that each side-window glass ruptures into more than 50,000 particles, and that most of the particles had a diameter of less than 0.01 in. Not all the particles separated as they dispersed and some heavier pieces, 2 to 3 in. in diameter, were seen accompanying this glass "cloud" as it shot across the car interior at speeds sometimes faster than that of the striking car. However, the average particle size of tempered glass is substantially less than that of laminated glass. Also, partial failures of laminated glass leave glass residuals bonded to the window frame that may be extremely hazardous to motorists contacting them. Head impact with side glass was discussed earlier.

Accidental Door Openings

For the twelve Series II intersection collisions (2), no door openings occurred for either car in the 10- or 20-mph collisions. One accidental door opening occurred for the struck car in the 30-mph collisions, but no doors opened for the striking cars. It was the left front door that opened for the car struck at its left front wheel by a 30-mph car. Four accidental door openings occurred in the 40-mph collisions, all in struck cars. To avoid misinterpretation of these findings, it is important to note that the adult dummies were restrained by safety belts in all but one of the twelve Series II experiments; the exception was one of the 40-mph crashes. This research positively established that door latch failures, with subsequent ejection of motorists are in part the result of the unrestrained motorist's body unavoidably hurled against the car door, in battering ram fashion, to contribute to door latch failure. Referring specifically to correlate Experiment 57, no doors opened, although the impact was directed to both doors on the left side of the struck car. In Experiment 62 the right front door of the struck car was forced open during the initial phase of the impact. At the instant that this right front door popped open, both front seat adult dummies were being forced against the left front door (Fig. 10), away from this opening door. Three conditions acting separately, or in combination, may account for this door opening against the transverse inertia forces of collision acceleration:

1. The front seat was pushed to the right against the right front door as the striking car crushed into its left side.
2. Tension-failure action of the latch, as a result of high car body bending forces during impact, undoubtedly contributed to door latch failure.
3. Possible reduced latch-holding efficiency as a result of the higher impact forces to which this car was subjected during a previous 40-mph collision experiment.

In connection with this last item, door latch failure as a result of prior impact exposures, this factor could not be unconditionally identified because of the other two factors operating and tending also to open the door. However, reduced latch-holding efficiency is the only feature of the three that is different from the conditions operating for X-57 wherein no door opened. Consequently, although facilitated by seat thrust and car body bending forces, the door opening for X-62 is considered to be the result of prior collision abuse. Special attention during repair to make sure door latch operation is restored to its original effectiveness is vitally important to subsequent passenger safety. Without belts, at least the front seat passenger of X-62 would have been ejected and quite likely run over by his own car. This statement is based on the observation that the front seat occupants are subsequently released from being displaced towards the left door and abruptly forced towards the open right door, while the car is side-skidding to a stop.

FINDINGS AND CONCLUSIONS

These findings and conclusions are abstracted from the text for the convenience of the reader; however, the statements apply only within the context of the section of the

paper from which they were abstracted. Any generalization of these findings and conclusions may lead to misinterpretations.

Vehicle Collision Dynamics and Damages

General

1. The intersection collision is among the most complex of motor vehicle collision exposures. The principal variables requiring consideration are speed, angle of impact, eccentricities of impact, the structural properties, and weights of the vehicles involved.

2. For right-angle collisions up to 40 mph, a car's collision performance is essentially unimpaired by damage sustained from previous collisions, providing quality repair work has been performed.

3. The automobiles involved in these correlate experiments were observed to follow approximately the same collision sequence of events, to approximate the same changes in direction and spin-out patterns, as well as to reach about the same positions of rest.

4. The correlate collision experiments provided almost perfect replication of the car resultant acceleration data. This close correlation supports the value of carefully controlled collision experiments.

5. Peak accelerations of 10G were obtained by the striking car in X-57 and in X-62, whereas the corresponding peak accelerations for the struck car were 16G and 17G. These observations take on added importance when making comparisons between the performance effectiveness for the different restraint configurations worn in X-57 and X-62.

6. Post-impact movement of vehicles involved in intersection collisions may be categorized as follows:

   (a) The car spins and then rolls on its wheels an additional distance before coming to rest, or
   (b) The car starts to spin at impact approaching a broadside skid (older models of cars may overturn at this point, as was observed in the Series I intersection collision experiments) as it comes to rest, or
   (c) The car's heading is altered by impact but it continues thereafter, to roll towards its position of rest.

Speeds at impact, position of impact and to a lesser extent the respective types of cars involved are the principal independent variables operating to modify collision dynamics.

7. The dispersal of collision debris covered approximately the same area for these correlate experiments. However, the centroid of the debris area was substantially remote from the point of impact.

Collision Generated Skids and Gouges

8. (a) Deviation skid marks, when correctly interpreted, are useful in identifying vehicle position on the roadway at the time of impact. A deviation skid mark is made only during collision:

      (1) As a result of the tire being abruptly stopped or nearly stopped by intruding structure of the opposing vehicle as the wheel is crushed rearward and frequently sidewise, or as a result of a side impact. When the brakes have been previously locked up, the deviation skid characteristics are most conspicuous, or
      (2) As a result of the distressed tire being overridden by the other colliding vehicle making the deviation skid blackest because this places additional load on that tire.

   (b) Non-braked brush skids are generated by tires on the advancing side of the arc that the center of mass of the car is following. Tires on the trailing side may carry a car load insufficient to generate observable rubber brush marks on the pavement. At times, these tires are entirely off the pavement.
   (c) In addition to car rim flanges, undersides of bumpers or fractured bumper

supports and underbody sill-metal or frames occasionally are forced into the pavement leaving gouge marks.

(d) Correlation of these pavement gouges with abraded metal components found on the wrecked vehicle often provide an objective basis for establishing the position of the car when those pavement gouges were generated.

(e) Pavement gouges may be made by the damaged vehicle at its position of impact, or on its way to its position of rest, or both.

Post-Impact Retardation of Vehicles

9. For these intersection collision experiments, the average coefficients of friction were calculated for the uniform, level, clean and dry asphalt surface on which the collision experiments were conducted by evaluating four-wheel locked skid tests made over the same speed range as used for the collision experiments.

(a) The average coefficient of friction for locked skidding was 0.75.

(b) When the car is in a broadside skid, the effective coefficient of friction may exceed the locked wheel skid coefficient of friction over the same surface. This will depend, however, on the extent of rim-gouging, which may occur even though the tires remain fully inflated, and also on whether the car body-sill contacts the pavement.

(c) Such car-metal-to-road contact will generate sparks that may induce post-collision fire and occasionally pavement scrape marks will be visible following the collision.

(d) This car-to-road contact is often more evident, however, by inspecting the car rim flanges and body-sill areas for pavement abrasions.

(e) Examples of specific value for the average effective coefficient of friction for cars primarily undergoing broadside skidding are $f = 0.7$ for the struck car of X-57, $f = 0.6$ for the struck car of X-58, and $f = 0.9$ for the striking car of X-61. The deviation of these values from the locked-skid coefficient of 0.75 for this surface has been explained in connection with car-metal-to-pavement contact and the other factors previously described as accompanying these intersection collisions.

(f) During spin-out, as the car's heading comes into alignment either with the direction (or the reverse direction) the car is moving, the effective coefficient of friction diminishes substantially—as would be expected. Crippled wheel suspension, collapsed frame structure, or driver braking may singularly or in combination act to prevent this coefficient from approaching zero.

Damage Patterns and Repair Costs

10. For these correlated experiments, and with respect to both the striking and struck cars, the location, extent, and nature of damage for the corresponding cars provided excellent correlation. Mutual intrusion for the striking car's windshield as it crushed towards the non-impacted side of the struct car measured 1.9 ft for X-57 and 2.0 ft for X-62. The collision damage sustained by the cars provides a good indication of the relative speeds of the cars at the instant of impact. However, other factors such as the relative weights of the cars, their impact configuration, and secondary or tertiary collisions must also be considered for speed evaluations.

11. With respect to cost of repairs, the average of three estimates received for the striking cars of X-57 and X-62 were $710 and $670, respectively; the corresponding struck car estimates were $830 and $970, respectively.

Door Latch Failure

12. Three conditions acting separately or in combination, may account for the door opening in X-62 against the transverse inertia forces operating during collision acceleration:

(a) The front seat was observed being pushed to the right against the right front door as the striking car crushed into its left side,
(b) Tension-failure action of the latch, as a result of excessive car-body bending forces during impact,
(c) Possible reduced latch-holding efficiency, as a result of the higher impact forces this car was subjected to during a previous 40-mph collision experiment.

13. Prior collision abuse, unless completely repaired, may lead to reduced door latch holding efficiency. With respect to X-62, although facilitated by seat thrust and car body bending forces, the reason the right front door opened for X-62 and did not open for X-57 was attributed to prior collision abuse. Special attention during repair to restore door latch operation to its original effectiveness is vitally important to subsequent passenger safety. Without belts, at least the front seat passenger of X-62 would have been ejected and quite likely run over by his own car.

Side-Window Glass

14. In these correlate experiments, tempered side-window glass performance was compared with laminated side glass.

(a) Tempered glass fracture extends almost instantaneously throughout the entire sheet and is generally accompanied by a complete dispersal of glass fragments.
(b) Laminated glass may fracture with the appearance of a single localized crack or it may fracture with a total breakage accompanied with varying amounts of fragment dispersal.
(c) The resistance that tempered glass exerts against a striking object terminates at fracture. Edge prestressing of tempered glass may rupture the glass prior to head impact or may lower the threshold for rupture by head impact.
(d) For laminated glass, impact resistance continues to function following fracture until the plastic interlayer is ruptured.

15. The following are three causes for side-window breakage during intersection collisions:

(a) Abrupt lateral acceleration of the window frame and glass into the motorist's head,
(b) Comparable action into the motorist's shoulder by the window sill, sufficient to prestress and break the window glass,
(c) Encroachment by the striking car into the struck car side below its window level, or direct contact with its window.

16. The impact of the driver's head shattered out the left front tempered window of the struck car during X-57; the corresponding laminated glass was fractured during X-62 but remained in place.

(a) The tempered glass accounted for 53G peak acceleration, whereas the laminated glass accounted for an 82G peak acceleration. Edge stressing during the initial phases of impact reached a value sufficient to crack the tempered glass and the glass ruptured out completely from its mount. A similar crack or series of cracks developing in the laminated glass did not appreciably diminish its resistance to head impact because the cohesive properties of the plastic interlayer continue to function following initial cracking.
(b) The UCLA-ITTE laboratory studies excluded edge stress concentrations that were identified with full-scale collision studies. Accordingly, the laboratory impact velocity corresponding to the full-scale exposures that produced a peak simulated head acceleration of 83G for laminated glass

produced a corresponding peak acceleration of 130G for tempered glass of the same thickness.

(c) The poor correlation between simulated head impacts of 53G for the full-scale crash, and 130G for laboratory study, provides additional data indicating the sensitivity of tempered glass to coincidental edge stressing during collision.

(d) The close correlation between the simulated head impact peak acceleration of 82G obtained by full-scale crash tests and the simulated head impact of 83G obtained by laboratory tests demonstrates the relative insensitivity of laminated glass to coincidental edge stressing during impact.

17. The following concern side-window glass breakage for these correlate experiments:

(a) The struck car side-window glass was tempered for Experiment 57 and both left rear and left front windows were shattered with greater than 50 percent of the glass dispersal forced inside of the car,

(b) In Experiment 62 under the same experiment conditions, laminated side-window glass was installed. Both front and rear side-window glass fractured extensively but remained in place, except for about 10 percent of the glass for the upper forward corner of the left rear window that dislodged and was found inside the rear seat compartment.

18. With respect to the tempered side-window glass failures, it was found that each side-window glass ruptures into more than 50,000 particles and that most of the particles had a diameter of less than 0.01 in. Not all of the particles separated as they dispersed and some heavier pieces, 2 to 3 in. in diameter, were seen accompanying this glass "cloud" as it shot across the car interior at speeds sometimes faster than that of the striking car. However, the average particle size of tempered glass is substantially less than that of laminated glass. Also, partial failures of laminated glass leave glass fragments bonded to the window frame that may be extremely hazardous to motorists contacting them.

Simulated Motorist Exposures

Adults

19. The kinematics and impacted forces of the anthropometric dummies for corresponding seat positions of these correlate experiments followed a consistent pattern except when influenced by varying types of motorist restraints or by differences in the car interior surfaces encountered.

20. For intersection-type collisions, the lap belt peak-load values may be expected to increase in a rather uniform manner for corresponding increases in impact velocity. Having a tensiometer at each end of the lap belt tends to compensate for the effects of lateral body loading components. This occurs because the tensiometer towards which the body is thrown may show a reduced tension, whereas the other unit, for this same body displacement, would show a correspondingly increased value.

21. Driver interaction with the car's interior provided valid comparative data for these correlate experiments inasmuch as the car's collision performance was found to be substantially the same despite a prior divergent history of collision.

22. Passenger shoulder strap tensiometer readings are valid only with respect to their specification of the tensile force acting at the doorpost anchorage. They do not indicate the actual force magnitude applied to the motorist, although they do provide a useful indication of the relative severity of collisions. The reasons for this limitation were set forth in the text.

23. When the motorist is seated next to the impacted side, his seat belt tensiometer values should not be regarded as realistic data for the following reasons:

(a) The motorist is pinned against the side of the car because of the abrupt acceleration the car receives from the striking car; minor variations in the snugness of his belt are likely to lead to substantial differences in readings obtained under otherwise comparable conditions,

(b) The initial lateral shift of the driver's hips towards the striking car will be restricted by the intrusion of the striking car and this form of restraint is not registered by the tensiometer,
(c) If intrusion is sufficient, the driver may be displaced in the direction the striking car is advancing, thereby developing tensiometer readings that reflect body displacement forced by the intruding car, rather than true body inertial forces,
(d) High-speed motion picture camera coverage showed one dummy shifting during impact to load the other dummy and their respective restraints would reflect an underload for the shifting dummy and an overload for the struck dummy.

24. The slip-link feature for the shoulder cross-strap and lap belt combination allowed hip inertial forces to be transferred, in part, to increase the restraint applied to the chest. As a consequence of this slip-link feature, in the majority of the UCLA intersection collisions directed toward the shoulder cross-strap belt side affording reduced protection, the dummy appeared to be, nevertheless, rather well restrained.

25. The right front seat occupant's sideward movement for the struck car of the two 30-mph correlate experiments was approximately the same for the dummy wearing a shoulder cross-strap and lap belt combination as for the dummy with only the lap belt. Some allowance should be made, however, for the reduced degree of spinal articulation common to anthropometric dummies as compared with their human counterparts.

26. In Experiment 62, the right front seat passenger of the struck car would subsequently have been ejected had he not been wearing a lap belt. Additional protection is provided during forced door openings when the motorist is wearing a shoulder strap and lap belt combination because his head and chest are restrained from flailing outside the protective cabin enclosure where direct impact with another vehicle or a fixed object may occur.

27. When the shoulder cross-strap is anchored to the center doorpost, substantially above shoulder height, severe neck lacerations can result from this strap functioning to restrain upper torso ejection. Accordingly, the upper anchorage point for this strap should not be above average shoulder height; this fact points out the importance of separately designed restraints for children.

Children Motorists

28. Simulated three-year-old and six-month-old children provided preliminary evaluation of several protective restraint configurations:

(a) Simulated children riding in the struck car were exposed to greater potential injury than when riding in the striking car.
(b) The rear seat passenger compartment provides a less hostile environment during these collisions than does the front seat area, primarily because of the adverse forces that the front seat adult may inadvertently apply to the child during collision. Additionally, the more lethal nature of driving controls and the instrument panel as contrasted with the upholstered rear seat compartment points up the other reason why the rear seat is safest for children.
(c) A child standing behind the front seat in the struck car during an intersection collision is subjected to probable extreme abuse. Under identical collision exposure conditions, except with the child dummy sitting in the center of the seat on a cushion and restrained by an adult-type lap belt, the child avoided direct contact by collapsing structures and collision forces were applied to the child through the restraint in a non-injurious manner.
(d) When the three-year-old child dummy stood behind the front seatback on the right side for the striking car, the exposure was substantially less than the comparable position for the struck car because the striking car was abruptly jerked to its left tending to pin the child against the right side of the car in a not too abusive manner. Had the struck car been traveling in the opposite direction, the child would have been thrown violently to her

left paralleling the front seatback. Inasmuch as the motorist does not choose the type of intersection collision he becomes involved in, it is not recommended that children be allowed to stand behind the front seatback.

Infant Motorists

29. For the infant up to six months old, a bassinet was observed to provide effective protection, particularly when its long axis paralleled the long axis of the car and when it was positioned behind the center of the front seatback. The tie-down straps provided with most bassinets, when properly attached, greatly increase infant protection during collision. Additional protection is afforded by the use of a covering such as a net to prevent the infant from being thrown out of the protective confines of the bassinet. Older children occupying the rear seat area should wear restraints not only for their own protection but also to prevent their being thrown against the infant's bassinet during impact.

30. Small children from about six months and older may receive adequate protection from well-designed restraining harnesses. The protective harness for small children should include the following features:

(a) A harness configuration that applies forces approximately equally to the shoulder and pelvic girdles.
(b) A slip-loop feature that permits the small child to stand, sit, or lie down on the seat while continuously restrained.
(c) An anchorage that prevents the seatback from shifting forward during impact. This anchorage can at the same time be used to limit the motion of the small child, but must be arranged to prevent the seat inertial forces from being applied to the child.
(d) Attachment of child restraints to the car seat should be made only where the car seat is anchored by special devices to the floor pan.
(e) Restraints that apply forces to the viscera or adjacent areas of the body midway between the pelvic and shoulder girdles are dangerous and unworthy of consideration.

Belt Elongation

31. For these intersection collision exposures no belt elongation or permanent set occurred. This was because the forces applied to the safety restraints did not approach the loop strength limits prescribed for these belts. These protective restraints met the strength requirements prescribed by SAE. Properly restrained, the 30-mph intersection collision is survivable, except possibly for motorists sitting next to the impacted side of the struck car.

Data Reduction

32. Reduction of large volumes of impact-type data has been successfully accomplished by computer techniques. The process of extracting the square root of the sum of the squares and several tens of thousands of triaxial data points, of applying the various channel-scaling factors and of regraphing to a common scale is a laborious task quite appropriate for the digital computer. The program that has provided satisfactory data reduction uses a sequence of overlapping parabolic curves for computer presentation of the accelerometer curve. This procedure enabled the computer to follow faithfully the sharp peaks occurring at irregularly spaced intervals that are characteristic of acceleration patterns generated during collision.

REFERENCES

1. Severy, D. M., Mathewson, J. H., and Siegel, A. W., "Automobile Head-On Collisions, Series II." SAE Trans., 67: 238-262 (1959).
2. Severy, D. M., Mathewson, J. H., and Siegel, A. W., "Automobile Side-Impact Collisions, Series II." Paper, Soc. of Automotive Engineers National Automobile Week Session, Detroit, Mich. (1962).

3. Severy, D. M., and Snowden, W. H., "A Review of the State of Knowledge and Research Concerning Laminated and Tempered Safety Glass in Motor Vehicles." Special Report, Institute of Transportation and Traffic Engineering, Univ. of Calif., Berkeley and Los Angeles (Nov. 1, 1962).
4. Radt, H. S., and Milliken, W. F., "Motions of Skidding Automobiles." Society of Automotive Engineers Preprint 205A (June 1960).